Illustrations

The plates illustrate a number of shapes now being produced. They are explained in the associated captions.

1 Whyte, L. L, Wilson, A. G and Wilson, D., *Hierarchical Structures*, Elsevier, New York, 1969.
2. Pauling, L. and Corey, R. B, *J. Am. Chem. Soc*, 1950, **72**, 5349
3 Kroto, H W and Walton, D. R M, *The Fullerenes*, Cambridge University Press, 1993
4. von Schnering, H. G. and Nesper, R., *Z. Phys*, 1991, **B83**, 407–412.
5 Bragg, W. L. and Lipson, H. S., *Z Kristallogr*, 1936, **95**, 323–337.
6 Mackay, A. L., *Chem Phys. Lett*, 1994, **221**, 317–321
7 Ewald, P. P, *Ann. Phys.*, 1921, **IV64**, 253–287
8 Fourcade, B., Mutz, M. and Bensimon, D., *Phys Rev Lett.*, 1992, **68**, 2551–2554
9. Fourcade, B, *J. Phys II France*, 1992, **2**, 1705–1724.
10. Köning, J, Boettcher, C., Winkler, H, Zeitler, E, Talmon, Y and Fuhrhop, J-H, *J. Am Chem. Soc*, 1993, **115**, 693–700
11. Andersson, S., Jacob, M. and Lidin, S., *Z Kristallogr.*, 1995, **210**, 3–4.

ACKNOWLEDGEMENTS I am most grateful to my colleagues, J. Klinowski, D. Cvijović and H. Terrones for help and for providing a number of pictures. Financial help for computing from the Royal Society and University of Paris–Sud has been most valuable and the hospitality of the Indian Institute of Science is particularly acknowledged

Received 12 June 1995, accepted 13 June 1995

Observed and theoretical acceleration response spectra in the Tehri region: Implications for seismic hazard in the region

K. N. Khattri

Wadia Institute of Himalayan Geology, 33, General Mahadeo Singh Road, Dehra Dun 248 001, India

This paper presents an estimate of the seismic hazard in the Tehri region of the Himalaya. Theoretical simulations of strong motion expected in the vicinity of the fault of a $M_s = 7$ earthquake are used in conjunction with observed strong motion data for the 1991 Uttarkashi earthquake to conclude that for such an earthquake the peak acceleration at Tehri can be ~ 0.8 g. The corresponding spectral acceleration at $T = 1$ s can be ~ 0.98 g. Analysis of the strain budget of the region and a finite probability of occurrence of a great earthquake ($M_s > 8$) in the next 100 years or so is estimated. The spectral acceleration (T ~ 1–2 s) in the near-field region of such an earthquake is estimated to be of the order of 1 g.

ESTIMATION of seismic hazard is ordinarily based on one-parameter characterization of ground shaking, such as peak ground acceleration, peak ground velocity or peak ground displacement. The maps specify values of the chosen parameter at various sites with a given probability of exceedance in a chosen time span. Such single-parameter descriptions are most appropriate for characterizing the damage potential to short-period structures. However, in assessing the damage potential to complex structures such as dams and power plants, where a range of periods of the main structure and the substructures are involved, the details of the strong ground motion histories are needed to estimate properly the seismic hazard. For the purposes of seismic hazard characterization, the information in strong-motion time history is transformed into response spectrum, which specifies the levels of expected spectral accelerations at various periods.

Modelling is a standard scientific technique used for identifying the essential features of natural phenomena. Models are used to extrapolate and predict phenomena in domains for which empirical observations may not be available, but are needed. This is especially true in strong-motion seismology, as relatively few strong-motion accelerograms have been recorded so far, and the expected strong-motion time histories in earthquake-prone zones are needed to determine the parameters for earthquake-resistant design of structures.

In this paper we use the composite source model to represent a hypothetical earthquake similar to the 1991 Uttarkashi earthquake ($M_s = 7$) placed near Tehri, and use wave propagation theory to simulate the strong ground motions at Tehri[1–3]. We compare the results with those recorded for the Uttarkashi earthquake and show that the simulated strong ground motions are realistic

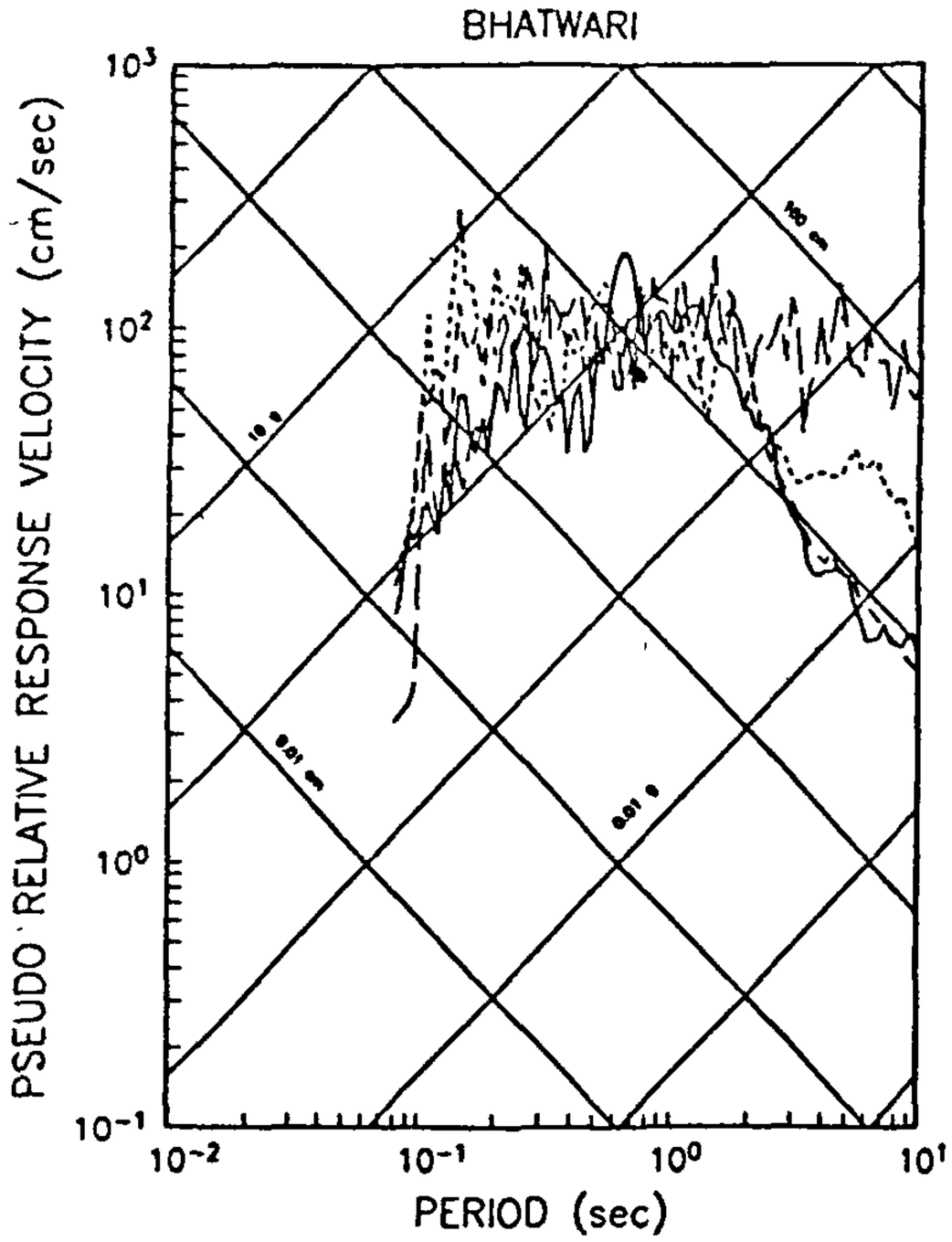

Figure 1. The observed pseudorelative response spectra at Bhatwari for the 1991 Uttarkashi earthquake ($M_s = 7$) are shown by solid line The synthetic spectra for Uttarkashi earthquake are shown by short dashes (no filtering of the synthetic accelerogram) and by intermediate dashes (filtering of the synthetic accelerograms with a filter equivalent to the one used in the observed accelerogram data processing The long dashes show the response spectrum for an $M_w = 8\ 5$ earthquake[2]. Note that the agreement between the observed and the synthetic response spectra is good for periods longer than 0 2 s. The damping in all cases is at 5%

We compute the response spectra for the simulated event, and compare them with the response spectra obtained at Bhatwari and Uttarkashi for the 1991 Uttarkashi earthquake. These sites were at comparable distances from the surface projection of the respective fault plane edge as was the simulated event from the surface projection of the fault plane edge of the hypothetical earthquake.

The magnitude of the most damaging earthquake that may strike the region in the next 100 years or so is also estimated using the available data on the past history of great earthquakes, the geological model of active tectonics in the region, and the strain rates obtained from a variety of geological and geophysical measurements as well as seismological data. The corresponding peak as well as spectral accelerations expected in the earthquake fault region are estimated. The peak accelerations expected on the basis of probabilistic analysis of seismological data are estimated and compared with those determined by the deterministic methods mentioned above.

The modelling procedure

The ground motions due to an earthquake depend on the position and nature of the earthquake source and the properties of the intervening medium; density, wave velocity and wave attenuation as a function of space coordinates. Knowing these parameters one can use the available theoretical frameworks to estimate the expected strong ground motions at a site.

Since earthquakes involve a complex process of rock fracturing, the procedure consists of representing the earthquake fault as a superposition of a large number of smaller circular subfaults distributed randomly over the earthquake fault plane. This models the heterogeneous nature of the earthquake faulting process. The number of subfaults with a given radius (R) is proportional to ($1/R^D$), where D is a fractal dimension. All subevents are assumed to have the same stress drop. Each subfault radiates a Brune source pulse[4, 5]. The sum total of moments of all the subfaults is constrained to equal the earthquake moment. The rupture is initiated at the hypocentre and sets off other subfaults as its rupture front expands and touches their centres. The elastodynamic radiation, for an appropriate model of earthquake source, is propagated to the site of observation by using numerically synthesized Green's functions for an appropriate layered earth structure. For $D = 2$, one obtains an ω^{-2} falling off of the spectrum at high frequencies of the elastodynamic radiation from a composite fault as used here. This is consistent with the empirical observations[6].

Results

Khattri *et al.*[2] and Yu *et al.*[3] used the above approach to model the strong ground motion records of the 1991 Uttarkashi earthquake and showed that the technique is able to reproduce the essential stochastic features of the observed data. The corresponding response spectra were also well matched over a wide range of periods. An example of this is shown in Figure 1. The response effects of the local (shallow) site geology, which is not known, is the most likely cause for the observed differences between the observed and the simulated spectral accelerations. Other factors that can contribute to the differences are inaccuracies in the velocity models used, as well as resonance effects of the severe topography in the region.

In this paper we use the above technique to estimate the nature of strong ground motions at Tehri expected for a hypothetical future earthquake of magnitude

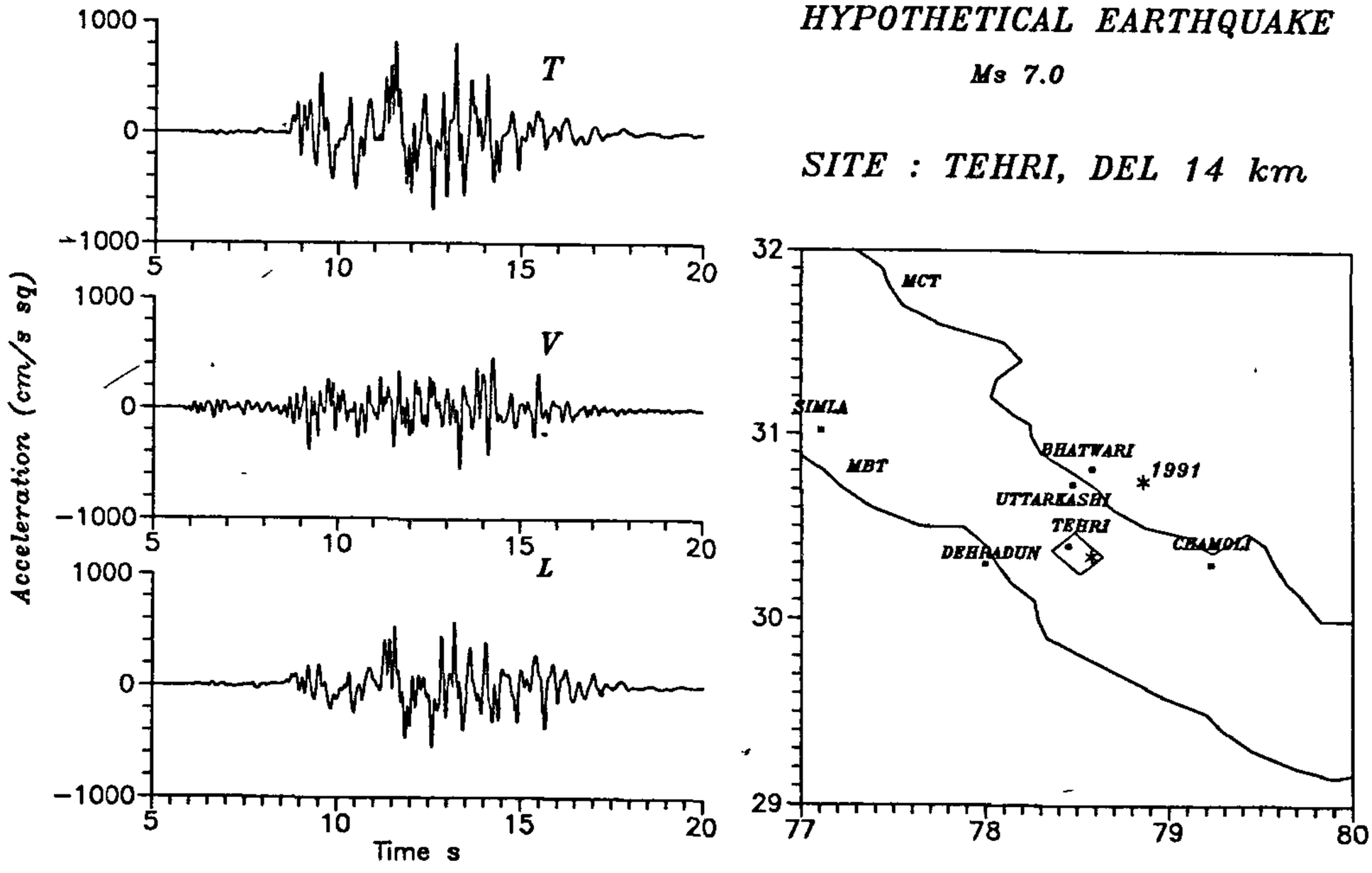

Figure 2. Accelerograms synthesized at Tehri for $M_s = 7$ earthquake. The location of the earthquake is shown as inset in Figure 3

$M_s = 7$, having similar fault plane solution and focal depth as the 1991 Uttarkashi earthquake. The fault plane of the hypothetical earthquake lies in the vicinity of Tehri, as shown in Figure 2. Tehri is located near the NW corner, but lies within the surface projection of the fault plane. The fault plane is located at a depth of 12 km with a dip of 14° towards NW. The strike of the fault plane is 317°. The area of the model fault plane is 16×24 km^2. This is based on the evidence for the 1991 Uttarkashi earthquake and the empirical relation available between fault dimension and the earthquake magnitude[7]. The slip is of thrust type, with the overthrusted block moving in an approximately SW direction. The velocity model used is shown in Table 1[2, 3]. Note that a top layer of low velocity is included in the model to represent a weathered layer, and (or) sediments. A stress drop of 30 bar is used in the simulation.

The synthetic acceleration time histories at Tehri for the transverse, vertical and longitudinal components are shown in Figure 2. The duration of strong shaking is approximately 8 s. The transverse component shows the largest value of 816 cm/s^2 for the peak acceleration. The peak acceleration values for the longitudinal and the vertical components, respectively, are 573 cm/s^2 and 537 cm/s^2. There is a lower-frequency component in these accelerograms which seems to separate the larger acceleration peaks.

Figure 3 shows the spectra of the acceleration time histories. The spectra show a corner at a frequency of about 0.02–0.04 Hz, which corresponds to a source dimension radius of ~8 km. This is consistent with the subfault size chosen for modelling the earthquake ground motions. At 10 Hz the sudden drop in amplitude is due to the computation of the Green's functions up to that frequency only.

The acceleration response spectra at 5% damping are shown in Figure 4. The highest spectral accelerations of about 2 g are observed in the short period range of 0.1–0.7 s. At a period of 1 s, the spectral acceleration value is ~ 1 g for the T component, ~ 0.7 g for the L component and ~ 0.3 g for the vertical component. At a period of 2 s, the spectral acceleration value is ~ 0.8 g for the L component, 0.55 g for the T component and ~ 0.2 g for the vertical component.

Table 1. Velocity and Q model

Thickness (km)	V_P (km/s)	Q_P	V_S (km/s)	Q_S	Density (g/cc)
0 4	3 5	50	2 00	25	1 80
1 0	5 0	80	2 86	50	2 40
15 0	5 2	4000	2 97	2000	2 60
30 0	6 0	4000	3 43	2000	2 90
Infinity	8 33	1000	4 83	500	3 30

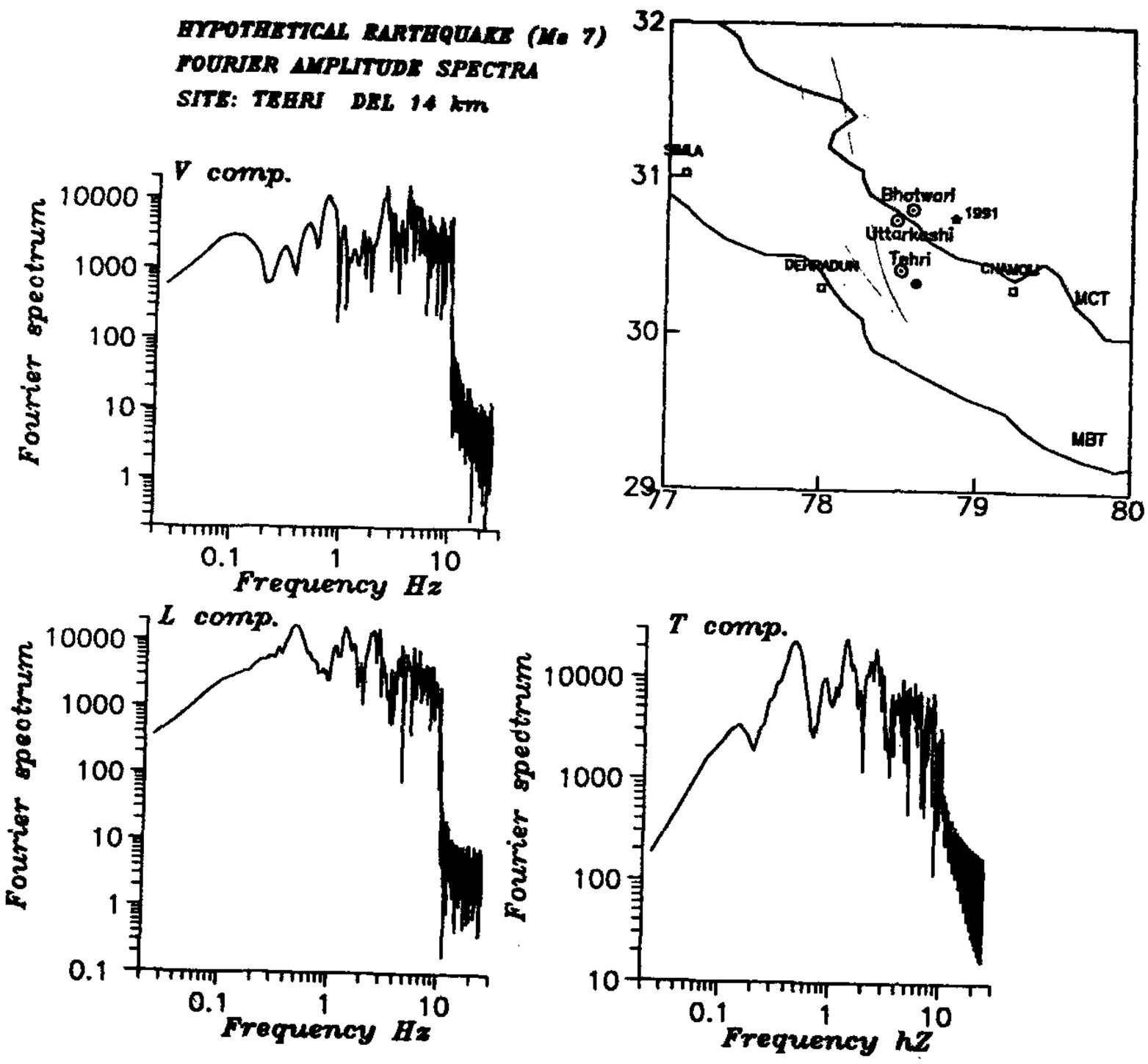

Figure 3. Fourier spectra of accelerograms synthesized for the site at Tehri

Discussion

Accelerations near the fault zone

We discuss the theoretical results obtained above in the light of the observed strong motions at Uttarkashi and Bhatwari for the 1991 $M_s = 7$ Uttarkashi earthquake. These sites are located close to (within about 2–10 km) the surface projection of the inferred fault plane. Also, they are located in the direction of rupture propagation. In the simulated model, the Tehri site is located over the surface projection of the fault plane, about 7 km inside it. It is also in the direction of rupture propagation.

The observed accelerograms for Bhatwari and Uttarkashi are shown in Figures 5 and 6, respectively. Bhatwari is at an epicentral distance of 25 km and Uttarkashi at 36 km. Although the epicentral distance loses its conventional meaning in the near field of the earthquake, it serves to provide a reference scale in terms of relative positions with respect to the fault plane as well as the fault dimension. The propagation effects will also be governed by this parameter. Peak accelerations of 0.24 g, 0.30 g and 0.19 g have been recorded for L, T and V components, respectively, at Uttarkashi. Similarly, peak accelerations of 0.25 g, 0.24 g, 0.29 g have been recorded for L, T and V components, respectively, at Bhatwari.

The peak acceleration represents the high-frequency component of the energy, and most of it will be contributed by the faulting process near the site. Since both Bhatwari and Uttarkashi are at similar distances from the fault edge, they are likely to have similar values of the peak accelerations. Such is indeed the case, as is documented above. However, at lower frequencies (longer periods) the contributions from the entire fault plane will be important, as they will become increasingly coherent with longer periods (wavelengths). Thus, the entire fault plane will contribute to the energy. The epicentral distance will also play a more significant role in determining the amplitude. This phenomenon can be observed better in the response spectrum.

The response spectra at Bhatwari and Uttarkashi are shown in Figures 7 and 8, respectively. We note that the shorter-period spectral responses (0.1–0.4 s) show comparable levels at the two stations, in keeping with simi-

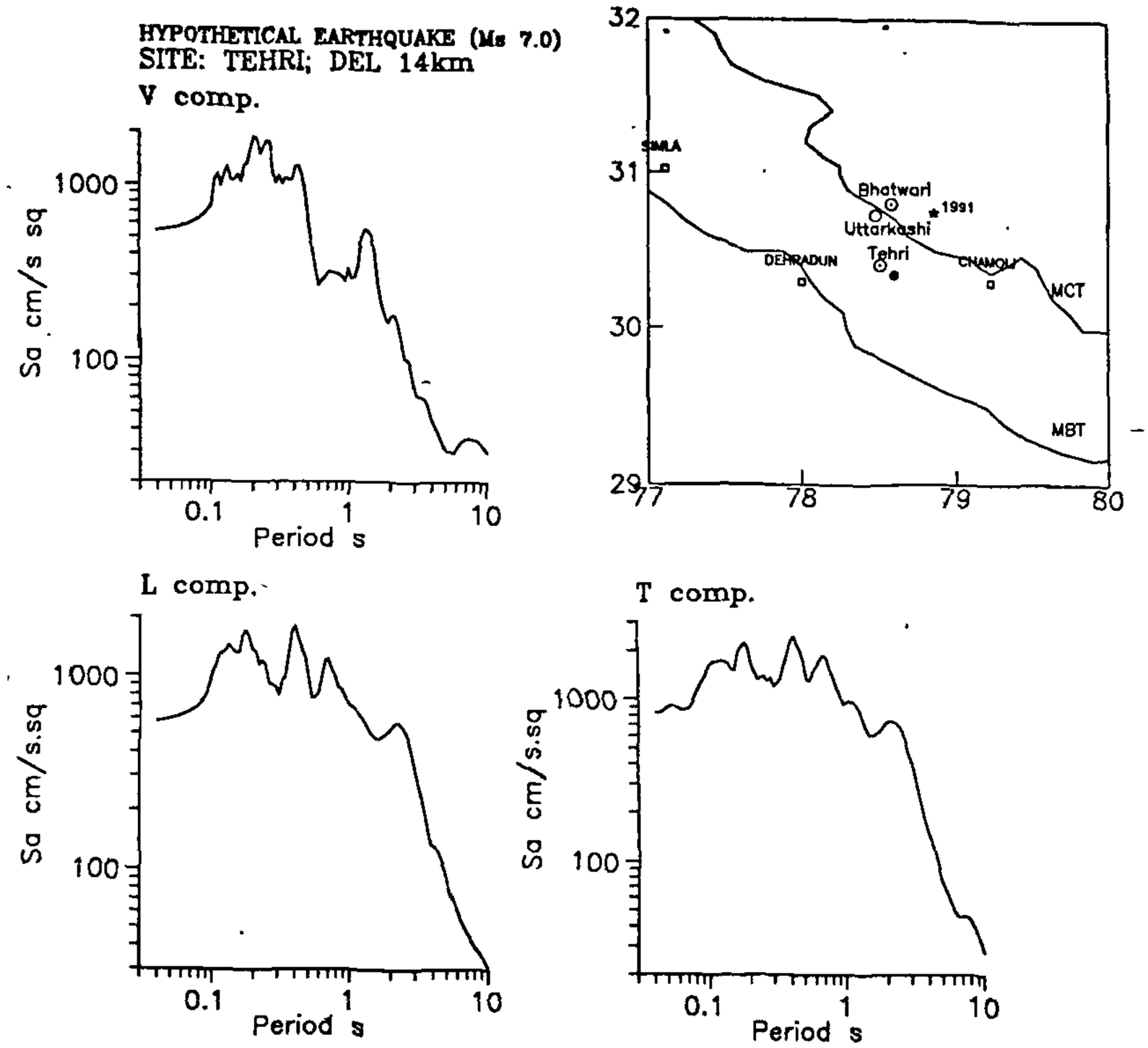

Figure 4. Response spectra at Tehri for 5% damping.

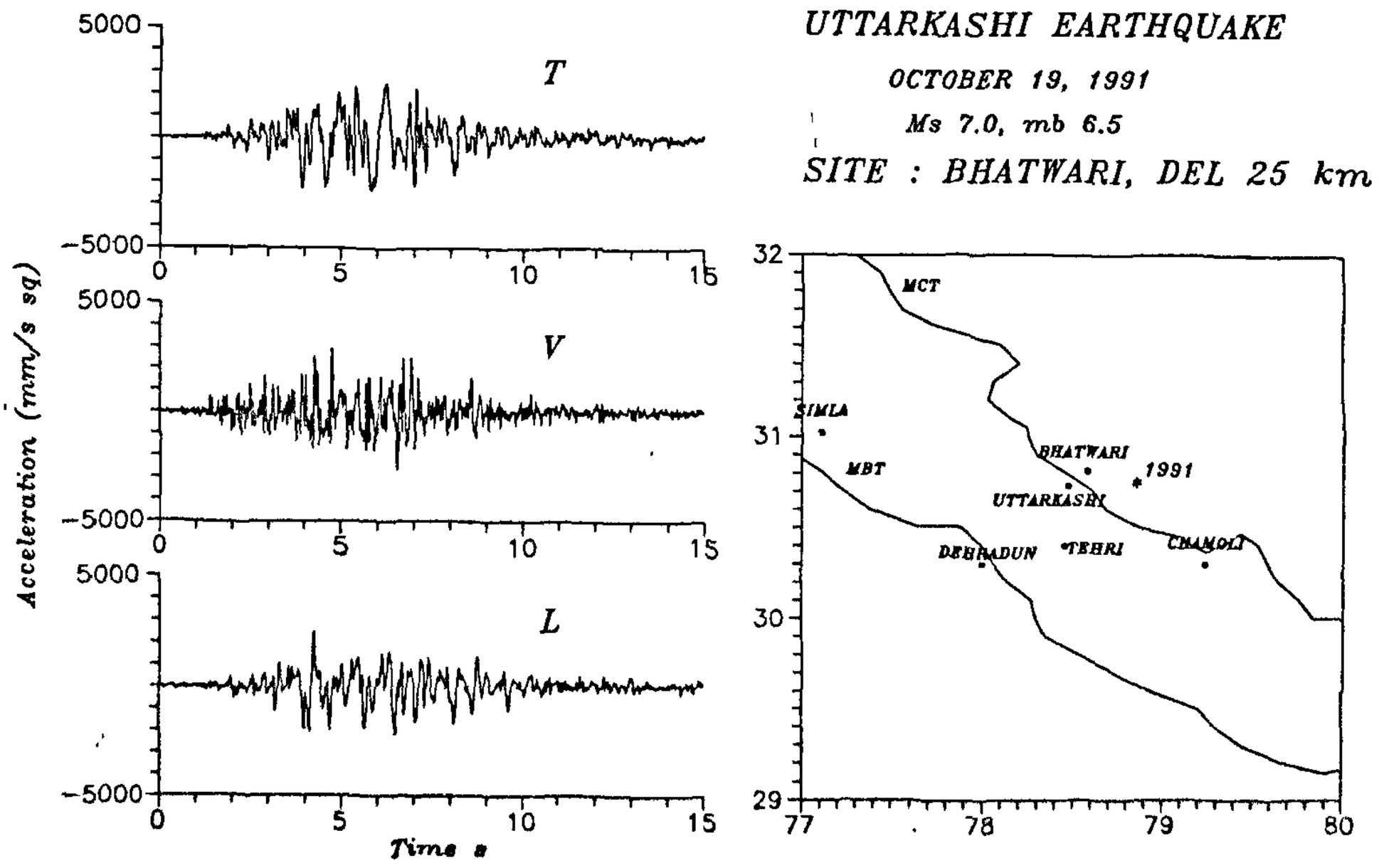

Figure 5. Accelerograms recorded at Bhatwari for the 1991 Uttarkashi earthquake (M_s = 7)

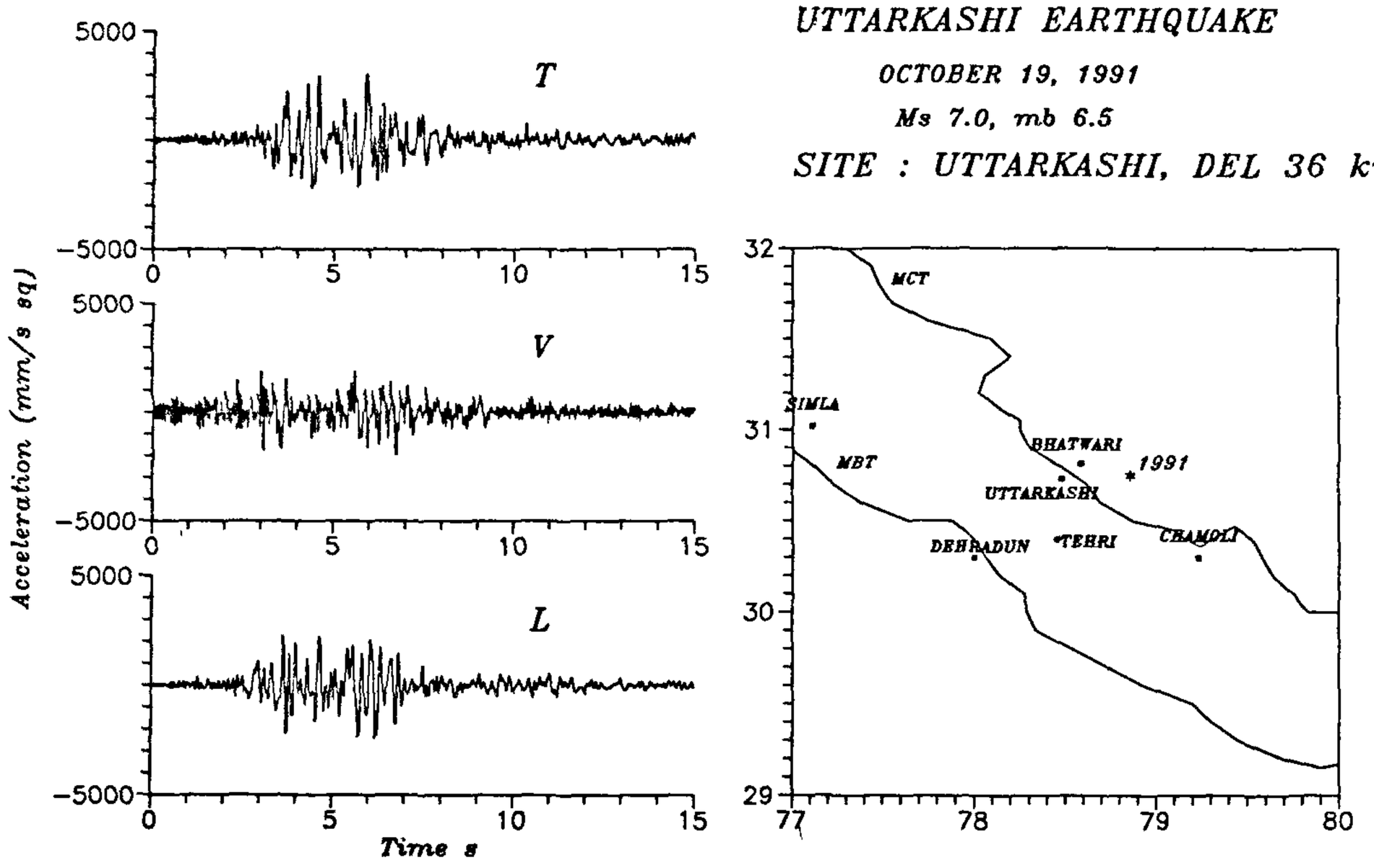

Figure 6. Accelerograms recorded at Uttarkashi for the 1991 Uttarkashi earthquake ($M_s = 7$)

lar observations for the peak acceleration values. However, the long-period spectral responses begin to show the effects of epicentral distance. For example, at ~ 1 s period, the spectral accelerations at Bhatwari and Uttarkashi are, respectively, 0.22 *g* and 0.10 *g* for the L component, 0.43 *g* and 0.18 *g* for the T component, and 0.11 *g* and 0.10 *g* for the V component. Similarly, at 2 s period, these values are 0.08 *g*, 0.03 *g* for the L component, 0.11 *g* and 0.04 *g* for the T component, and 0.06 *g* and 0.05 *g* for the V component. We notice a falling off of spectral acceleration amplitudes for the horizontal components by a factor of about 3 at these longer periods for a change of epicentral distance from 25 km for Bhatwari to 36 km for Uttarkashi, i.e. an increase of 11 km.

Let us now consider the results obtained for the case of simulation for Tehri. As noted above, peak accelerations of 0.82 *g*, 0.57 *g* and 0.53 *g* have been obtained for T, L and V components, respectively. The largest value is higher by a factor of about two-and-a-half compared to the observed value at Uttarkashi. This increase is theoretically anticipated on account of the smaller distance of Tehri to the fault plane, its smaller epicentral distance (~ 14 km), as well as resonance effects of the near-surface low-velocity layer at Tehri.

The estimated spectral accelerations at Tehri are about 3 to 4 times those observed at Bhatwari for periods up to ~ 1.7 s. At 2 s period, an amplification by 7 has also been observed. In general, the scaling is increasing for longer periods both for the empirical data set (from Uttarkashi to Bhatwari) as well as in the synthetic case (from Bhatwari to Tehri). As discussed above, this is a consequence of increasing coherency of the elastodynamic radiations at longer periods. The scaling by a factor of 3 to 4 is consistent with similar scaling observed between Bhatwari and Uttarkashi for a reduction of 11 km in the epicentral distance. The epicentral distance reduction for Tehri is 10 km with respect to the epicentral distance for Bhatwari. The various data described and discussed above are given in Table 2. The systematic dependence of the spectral accelerations on the epicentral distance discussed above is shown in Figure 8.

The synthetic strong-motion histories are consistent with the observed data at Bhatwari and Uttarkashi for the 1991 Uttarkashi earthquake. They have the appropriate amplitude envelope, duration and frequency characteristics. However, as discussed above, the observations at Bhatwari and Uttarkashi do not provide a suitable basis of estimate of the peak acceleration at Tehri, as both these sites were outside the fault zone; secondly, the Tehri site is well within the fault zone in the model calculations; and thirdly, it includes a low-velocity layer at a shallow depth, which will introduce

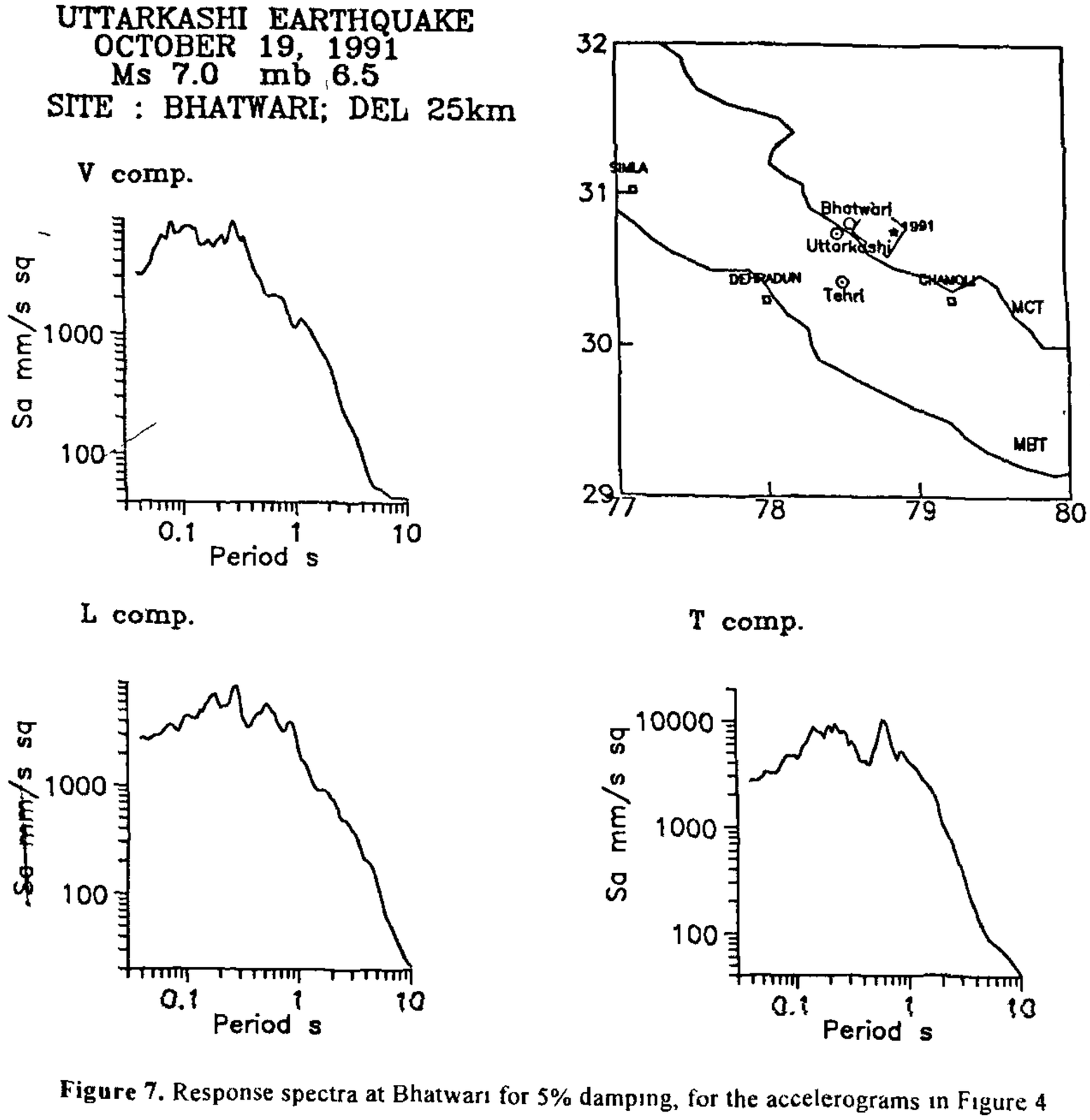

Figure 7. Response spectra at Bhatwari for 5% damping, for the accelerograms in Figure 4

resonance effects at shorter frequencies. Such a layer is not expected to exist at either Bhatwari or Uttarkashi, both of which are located adjacent to the High Himalaya having a very high rate of erosion. But such a layer is expected to be present at Tehri as indeed brought out from the analysis of the strong motion data for the Uttarkashi earthquake[3]. Furthermore, peak ground accelerations of about 1 g near the faults have been recorded in several earthquakes[8, 9]. Therefore, the maximum peak acceleration of 0.82 g obtained for the T component is a realistic estimate.

The observed data as well as the foregoing analysis indicate that the synthetic accelerograms and the corresponding response spectra for the Tehri site represent a realistic seismic hazard scenario for the type of earthquake and the site under consideration.

Estimation of the most damaging future earthquake in the Tehri area within the next about 100 years

Estimation of seismic hazard in a region depends on the most damaging earthquake that can occur in the region in the time window under consideration. This is illustrated by considering the accelerations expected for large earthquakes. For example, the Idriss[10] formula provides the following estimates for acceleration values for the cases of $M = 8$ and $M = 8.5$ earthquakes at distances of 15 and 25 km (see Table 3).

Table 3 shows two things. First, *there is a drastic increase in the expected acceleration amplitudes as we go from $M = 8$ to $M = 8.5$. Secondly, the high values of the spectral accelerations imply a long duration of shaking with high acceleration values.*

An estimate of the peak acceleration acquires significance when, as is often the case, the seismic response spectrum based on site-specific observational data is not available. In such situations, the amplitudes of the response spectrum are scaled by anchoring the spectral acceleration at zero period of a standard mean level spectra, at the level of the peak acceleration expected for the site, or a parameter based on the same. However, alternative new techniques based on sound theoretical models, such as the one presented here, have now become available to provide estimates of the expected strong ground motion time histories and the corresponding response spectra.

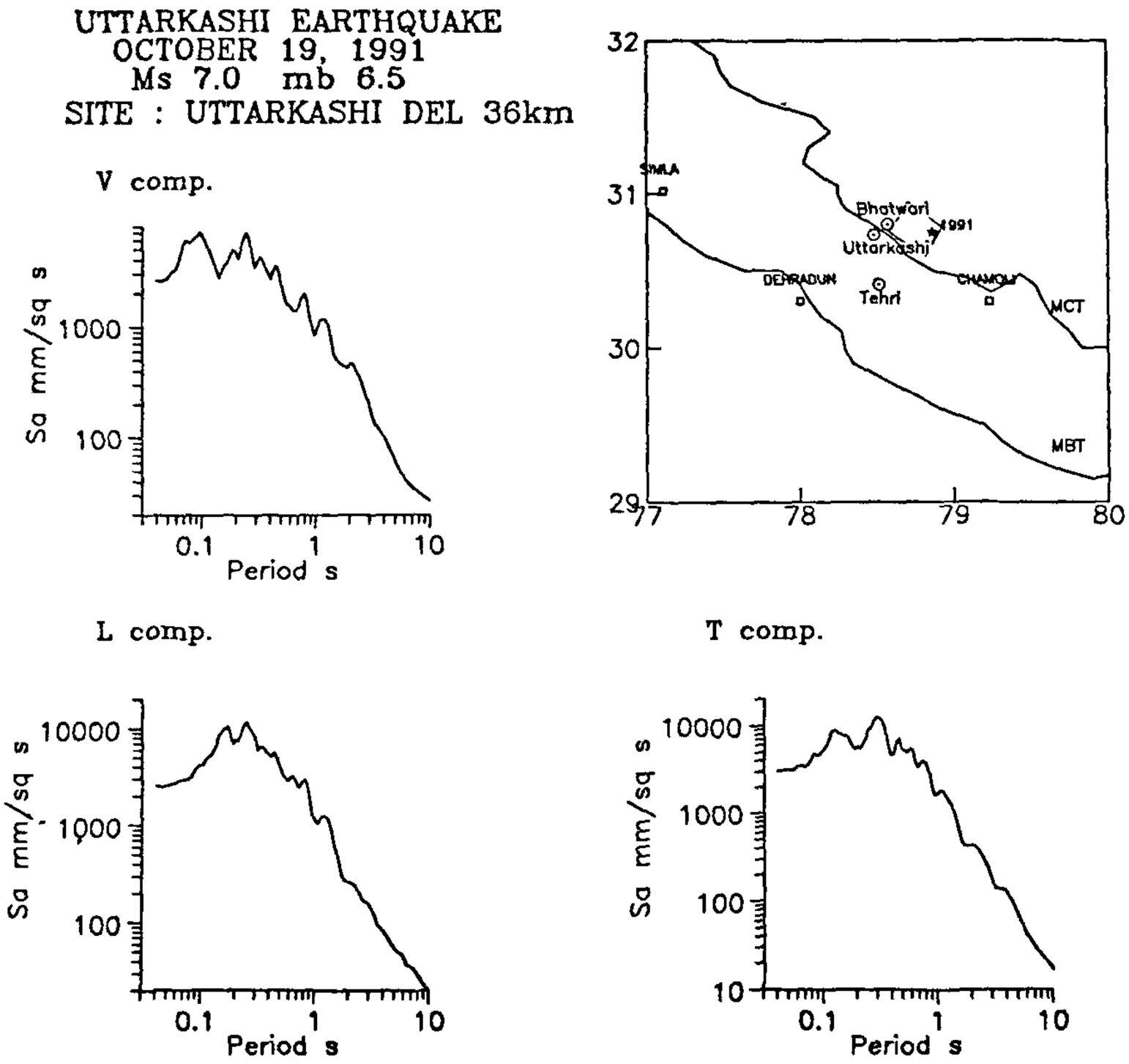

Figure 8. Response spectra at Uttarkashi for 5% damping, for the accelerograms in Figure 5.

The Himalayan belt is one of the most actively deformed zones on earth[12, 13], formed as it is by a succession of processes of strain accumulation and its catastrophic release in the form of earthquakes. The region has experienced four great earthquakes in the past about 100 years, namely, the 1897 Assam earthquake ($M = 8.7+$), the 1905 Kangra earthquake ($M = 8.6$), the 1934 Bihar–Nepal earthquake ($M = 8.4$), and the 1950 Assam earthquake ($M = 8.7$). The occurrence of peak accelerations in excess of 1 g in the great 1897 Assam earthquake has been well documented[14]. Since the geological process of the collision of the Indian plate with the Eurasian plate continues, causing persistent accumulation of strain, it makes certain that such great earthquakes in the Himalaya will continue to occur in the future.

An appraisal of the average return period of the $M = 8+$ earthquake in the region is, therefore, pertinent to the problem of seismic hazard estimation. This can be based on the strain budget of the region. The frequency of great earthquakes is constrained by the rate of strain accumulation in the region. The rate of strain accumulation has been estimated using a variety of techniques. The average rate of plate convergence obtained from marine magnetic anomalies is 5 cm/annum[15]. However, a fraction of this is transferred to the region north of the Himalaya. Thus, it sets an upper limit on the rate of strain accumulation in the region. Using the deformation of the upper Tertiary sediments in the Ganga foredeep, the average rate of strain is estimated to be 1.0–3 cm/annum in the western parts of the Himalaya[16, 17]. In the U.P. part of the Ganga foredeep, the average rate of convergence estimated from the velocity of the southward onlapping of the Indian shield is 1.8 ± 0.4 cm/annum[18]. The elastically stored component of the average rate of convergence estimated by using the rate of seismic moment released by great earthquakes in the Himalaya is 1.7 ± 0.3 cm/annum[19]. This strain becomes available for causing future earthquakes in the region. Using the fractal description of earthquake occurrences together with the complete catalogue of earthquakes, the average rate of slip over the basement thrust in the Himalaya has been estimated to be 3.5 cm/annum[20]. This rate will be approximately equal to the average rate of

Table 2. The values of peak accelerations and S_a (g)

Site Epicentral Distance (km)	Uttarkashi (observed) 36			Bhatwari (observed) 25			Tehri (synthetic) 14		
Component	T	V	L	T	V	L	T	V	L
a_p (g)	0 30	0.19	0 24	0.24	0 29	0.25	0 82	0 53	0 57
Factor				~ 1 5	~ 1	~ 1	~ 4	~ 2	~ 2
S_a (g) at $T = 0$ 98 s	0 11	0 16	0.08	0 30	0 47	0 12	0 70	0 96	0 33
Factor				~ 3	~ 3	~ 1 5	~ 2 5	~ 2	~ 3
S_a (g) at $T = 1$ 04 s	0.10	0 18	0.10	0 22	0 43	0.11	0 69	0 98	0 29
Factor				~ 2	~ 2	~ 1	~ 3	~ 2	~ 2 5
S_a (g) at $T = 1$ 23 s	0 12	0 14	0.12	0 16	0.36	0 13	0 61	0 85	0 50
Factor				~ 1	~ 2.5	~ 1	~ 4	~ 2	~ 4
S_a (g) at $T = 1.50$ s	0 05	0.06	0 05	0 09	0.26	0 09	0 48	0 60	0 41
Factor				~ 2	~ 4	~ 2	~ 5	~ 2	~ 5
S_a (g) at $T = 1.70$ s	0 03	0 04	0 04	0 09	0 21	0.08	0 49	0 65	0 21
Factor				~ 3	~ 5	~ 2	~ 5	~ 3	~ 3
S_a (g) at $T = 2$ 00 s	0 03	0 04	0.04	0 08	0 11	0.06	0 54	0 76	0 18
Factor				~ 3	~ 2 5	~ 1	~ 7	~ 7	~ 3

'Factor' represents the amplification factor with respect to Uttarkashi in the case of Bhatwari and with respect to Bhatwari in the case of Tehri

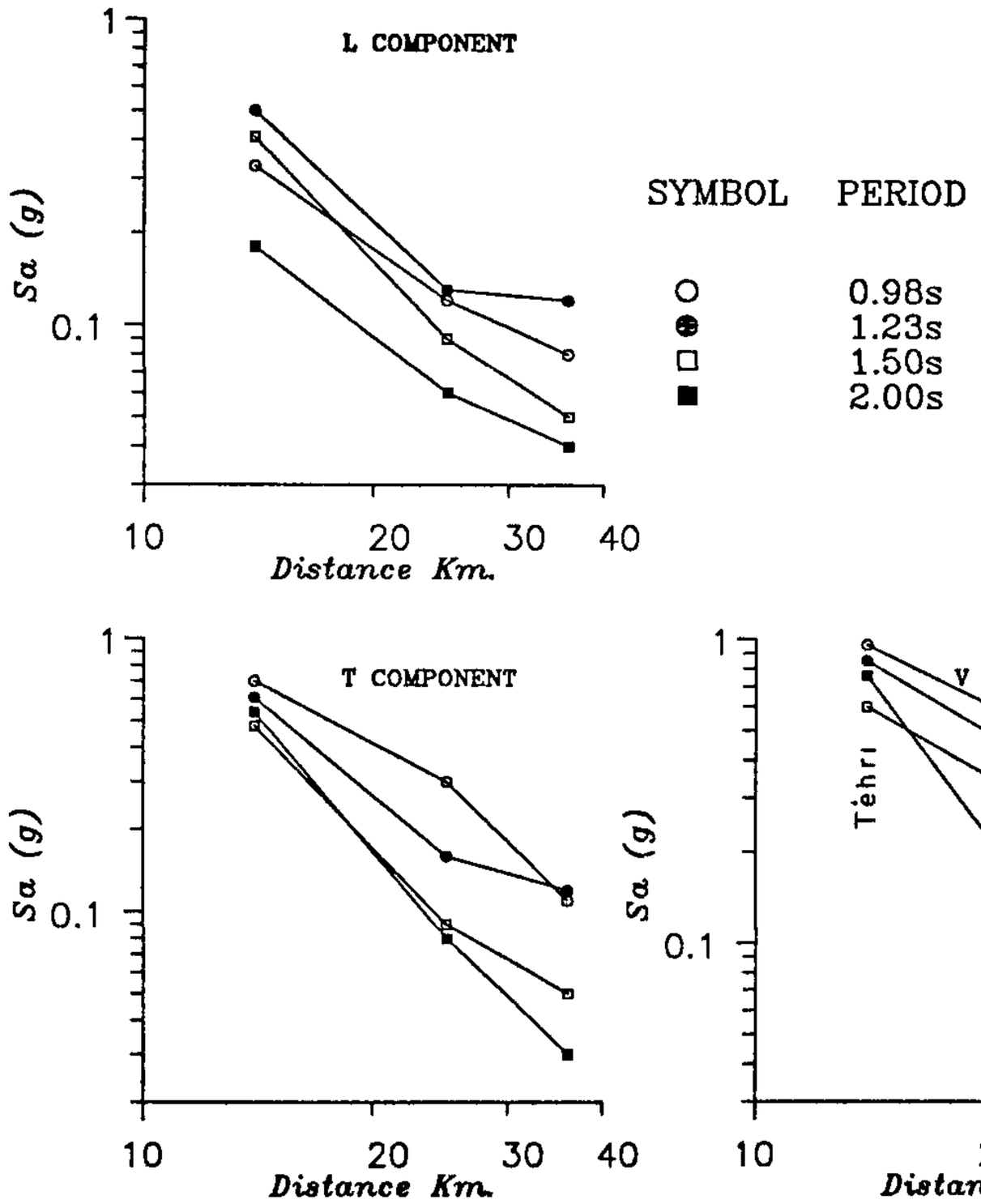

Figure 9. The variation of spectral accelerations as a function of distance and period The data used are summarized in Table 2

convergence in the Himalaya. Geodetic measurements using levelling in Dehradun and Kathmandu areas have been analysed to provide an estimate of the average rate of elastic strain accumulation to be 0.7 cm/annum in the outer Himalayan region[21]. The GPS measurements in Nepal have led to an estimate of the convergence rate of 1 ± 1 cm/annum[22].

From the foregoing discussion it is clear that the average rate of convergence in the Himalaya lies in the range of 1–3 cm/annum. The rate may vary along different

Table 3. Acceleration values using Idriss formula[10], quoted from Liam-Finn[11]

	$M = 8$		$M = 8.5$	
	$R = 15$ km	$R = 25$ km	$R = 15$ km	$R = 25$ km
a_p	0.66 g	0.485 g	0.75 g	0.575 g
a_{sp} at $T = 0.3$ s	2.1 g	1.6 g	2.5 g	2.0 g
a_{sp} at $T = 1.0$ s			1.14 g	
a_{sp} at $T = 1.2$ s			0.96 g	
a_{sp} at $T = 1.5$ s			0.75 g	
a_{sp} at $T = 2.0$ s	0.44 g	0.31 g	0.57 g	0.41 g

sections of the Himalaya. This can be revealed by detailed investigations using modern techniques like the GPS.

If one considers the average rate of elastically stored convergence to be 2 cm/annum then sufficient strain will become available in any sector of the Himalaya to generate a great earthquake in a period of about 500 years. In the sector in front of the Salt range, where the rate has been estimated to be 1 cm/annum, the average return period will be correspondingly longer. In the sector containing the Pir Panjal Range, where the rate of convergence is estimated to be 3 cm/annum, the average return period is anticipated to be shorter. In the central gap region the estimated rate of convergence is close to the average value. Therefore, the 500-year return period is quite representative.

The four great earthquakes in the Himalaya over the past 100 years have between them relieved the accumulated strain in about 35% of the Himalayan plate boundary. The remaining sections of the Himalayan plate boundary have not experienced a great earthquake for the past at least 300 years, possibly 500 years or more. Thus, these sections, constitute veritable seismic gaps, with a large amount of accumulated strain, and are, therefore, places of high seismic potential for a future great earthquake in the next 100–300 years or so. The Tehri dam site lies in one such gap (Central gap)[23, 24], for which the shorter time interval applies.

It is also relevant to consider peak accelerations in the Himalaya, estimated using the standard probabilistic seismic hazard analysis[25]. The peak accelerations expected in the Lesser Himalaya (where the dam is sited) are $0.7^{+}g$ for a one in ten chance of exceedance in any time window of 50 years. When this is translated to a 100-year exposure period, the a_p value scales to about $0.9g$ (ref. 26).

The analysis of both the seismological and the strong-motion data are consistent in estimating that for the case of a great earthquake both the peak and the spectral accelerations ($T \sim 1$ s) in the fault zone in the Tehri region are expected to be around $0.9g$.

Conclusions

Recapitulating, the following conclusions emerge from the present investigation.

1. The observational strong-motion data for the 1991 Uttarkashi earthquake ($M_s = 7$) show that spectral accelerations of $0.43g$ ($T = 1.04$ s), $0.36g$ ($T = 1.23$ s) and $0.26g$ ($T = 1.5$ s) have been recorded at an epicentral distance of 25 km.

2. The corresponding synthetic strong motions for a hypothetical $M_s = 7$ earthquake at an epicentral distance of 14 km and located within the surface projection of the fault zone are $0.98g$ ($T = 1.04$ s), $0.85g$ ($T = 1.23$ s) and $0.60g$ ($T = 1.5$ s).

3. The spectral accelerations in the 1–2 s period range, estimated from model simulation at Tehri for the case of an $M_w = 8.5$ earthquake situated under Tehri at a depth of 12 km, are $\sim 1g$ (refs. 7, 8).

4. The Idriss[10] as well as the Campbell[27] empirical formulae also give spectral accelerations ($T = 2$ s) at 15 km distance to be at least $\sim 0.57g$ for an $M = 8.5$ earthquake. The acceleration will be higher at a closer distance of 12 km.

5. The rate of strain accumulation in the Central Gap (where Garhwal is situated) is around 2 cm/annum, which provides enough strain accumulation to generate a great earthquake in about 500 years. Since there has been no great earthquake in this gap for at least about 300 years and perhaps 500 years, the region (Central Gap) must be ripe for a great earthquake in the next 100 years or so. Of course, it is possible that the accumulated strain is initially released partially in a number of $M = 7$ or so earthquakes, instead of a single great earthquake ($M > 8$). In this case the occurrence of the great gap-filling earthquake will at best be somewhat delayed, but not forestalled. However, the scenario historically repeated by all great earthquakes in the Himalaya is the most appropriate basis for estimating seismic hazard.

6. The probabilistic seismic hazard analysis of the Himalaya shows that in any 100-year time window the probability of exceeding a peak acceleration of $\sim 0.9g$ in the Garhwal Himalaya is 0.1.

7. The above estimates of the seismic hazard characterization are consistent with the currently available corpus of geological, geophysical, seismological and earthquake strong-motion data. Therefore, it would be prudent to heed these estimates while scientifically evaluating the soundness of the aseismic design of large critical structures in the region.

8. There is a very high level of seismic hazard in the seismic gaps and in adjacent areas to their south with their densely populated centres. A systematic implementation of a well laid-out hazard mitigation plan is urgently called for.

1. Zeng, Y., Anderson, J. G and Yu, G , *Geophys. Res. Lett* , 1993, **21**, 725–728
2. Khattri, K N., Yu, G., Anderson, J., Brune, J. and Zeng, Y., *Curr Sci.*, 1994, **67**, 343–353.
3 Yu, G., Khattri, K N , Anderson, J., Brune, J. and Zeng, Y., *Bull. Seismol Soc. Am.*, 1995, **85**, 31–50.
4 Brune, J. N , *J Geophys. Res* , 1970, **75**, 4997–5009.
5. Brune, J N , *J. Geophys Res.*, 1971, **76**, 5002
6 Frankel, A , *J Geophys Res* , 1991, **96**, 6291–6302.
7. Kasahara, K., *Earthquake Mechanics*, Cambridge University Press, New York, 1981, pp. 19, 56–57
8 Brune, J. N., *Tectonophysics*, 1993, **218**, 281–286.
9 Ambraseys, N. N , in *Earthquake Hazard and Large Dams in the Himalaya* (ed Gaur, V. K.), INTACH, New Delhi, pp. 111–115
10 Idriss, I. M , Selection of earthquake ground motions at rock sites, Report prepared for the Structures Division, Building and Fire Research Laboratory, National Institute of Standards for Technology, Department of Civil Engineering, University of California, Davis, 1991.
11. Liam-Finn, W. D , *Earthquake Hazard and Large Dams in the Himalaya* (ed Gaur, V. K.), INTACH, New Delhi, pp 116–136
12. Valdiya, K S., in *Earthquake Hazard and Large Dams in the Himalaya* (ed. Gaur, V. K.), INTACH, New Delhi, pp. 1–34.
13. Nakata, T., in *Tectonics of the Western Himalayas* (eds Malinconico, L. L. (Jr) and Lillie, R. J), Geol. Soc. America Spl. Paper, 232, pp. 243–264
14. Oldham, R. D., *Mem. Geol. Surv. India*, 1899, **26**, 1–379.
15. DeMets, C., Gordon, R G., Argus, D. F. and Stein, S., *Geophys. J. Int* , 1990, **101**, 425–478.
16 Burbank, D W and Raynolds, R. H G., *Nature*, 1984, **311**, 114–118
17 Baker, D. M., Lillie, R. J , Yeats, R. S., Johnson, G D , Yousuf, M. and Zamin, A. S H., *Geology*, 1988, **16**, 3–7.
18 Lyon-Caen, H and Molnar, P., *Tectonics*, 1985, **4**, 513–538.
19. Molnar, P. and Pandey, M R., *Proc. Indian Acad. Sci. (Earth and Planet. Sci)*, 1989, **98**, 25.
20. Khattri, K. N , *Curr Sci.*, 1995, in press.
21. Chander, R and Gahalaut, V. K., *Curr Sci* , 1994, **67**, 531–534
22. Bilham, R. and Jackson, M , *J Nepal Geol Soc.*, 1994, **10**, 18
23. Khattri, K. N. and Tyagi, A. K., *Tectonophysics*, 1983, **96**, 281–297.
24 Khattri, K N., *Tectonophysics*, 1987, **138**, 79–92
25 Khattri, K. N , Rogers, A M , Perkins, D. M. and Algermissen, S. T., *Tectonophysics*, 1984, **198**, 93.
26. Khattri, K. N , Rogers, A. M. and Perkins, D M., *Bull. ISET*, 1983, **20**, 1–22
27. Campbell, K. W , *Himalaya with References to Tehri Dam, in Earthquake Hazard and Large Dams in the Himalaya* (ed Gaur, V. K.), INTACH, New Delhi, pp. 93–103.

ACKNOWLEDGEMENTS This research was supported by the Emeritus Scientist Scheme of the CSIR and the WIHG, who have kindly hosted me. I am indebted to Y. Zeng, G. Yu, and J. Anderson for allowing the use of their codes Thanks are due to G. Yu, who kindly ran some simulations, and to Sri Ram for running some graphics. I have benefited immensely from discussions with Professors V. K. Gaur, R. Chander and R. N Iyengar.

Received 12 May 1995, revised accepted 17 May 1995

Sr isotopes in rivers of India and Pakistan: A reconnaissance study

J. R. Trivedi, Kanchan Pande, S. Krishnaswami and M. M. Sarin

Physical Research Laboratory, Ahmedabad 380 009, India

It is well established[1] that the isotopic composition of Sr in sea water has oscillated on different time scales during the past ~600 Ma. These oscillations result from changes in the relative contributions of dissolved Sr to sea water from its two major sources, continental weathering and hydrothermal interactions, with their characteristic $^{87}Sr/^{86}Sr$. The continental input via fluvial weathering is generally more radiogenic (average $^{87}Sr/^{86}Sr$ 0.7119 ref. 2) compared to the hydrothermal $^{87}Sr/^{86}Sr$ of 0.7035 (ref. 2). The Sr flux and $^{87}Sr/^{86}Sr$ of different river systems vary widely[2–4] and in some way are related to the lithology of the drainage basin, the intensity of weathering and the efficiency with which they transport their dissolved load. We have measured the dissolved Sr concentrations and $^{87}Sr/^{86}Sr$ of the major rivers draining India and Pakistan. These measurements provide data on the flux of Sr isotopes transported by these rivers to the ocean and their impact on the Sr isotope evolution of the oceans. Further, as the river basins sampled comprise a diverse set of lithologic, tectonic and climatic regimes, they provide an opportunity to study the controls of these factors place in determining the Sr isotopic systematics of rivers.

THIS work forms a part of our geochemical reconnaissance study of the Indian rivers. Major ions, Sr and U isotopes were the principal constituents measured in the samples, the results of some of our earlier work are published elsewhere[5–9]. Figure 1 shows the sampling sites.

The rivers sampled can be conveniently classified into two groups[10,11] in terms of their basin geology, tectonics and climate – the peninsular and the extrapeninsular (Himalayan). The peninsular region is a tectonically quiescent shield area that has several mountain systems such as the Aravallis, the western and eastern Ghats and the Nilgiris, most of which are geologically mature This shield is made of Pre-Cambrian rocks of diverse origin,